

In the Name of God



Shiraz University
Faculty of Engineering

Ph.D. Dissertation
In Materials Science and Engineering

**Production of nickel-free stainless steel coated with
ZrTiO₄-PMMA hybrid sol-gel films and investigation
of its structure and electrochemical behavior**

**By
Erfan Salahinejad**

**Supervised by
Dr. Mohammad Jafar Hadianfard**

February 2013

In the name of God

Declaration Form

I, **Erfan Salahinejad**, a Materials Science and Engineering student from the faculty of Materials Engineering of Shiraz University, declare that this thesis is the result of my research and I have written the exact references and indication whenever I used others' sources. I also declare that the research and the topic of my thesis are not reproductive and guarantee that I will not disseminate its accomplishment and not make then accessible to others without the permission of the university. According to regulations of the metal and spiritual ownership, all rights of this belong to Shiraz University.

Name: Erfan Salahinejad

Date: 2/29/2013

Signature: *Salahinejad*

IN THE NAME OF GOD

**PRODUCTION OF NICKEL-FREE STAINLESS STEEL COATED WITH
ZrTiO₄-PMMA HYBRID SOL-GEL FILMS AND INVESTIGATION OF
ITS STRUCTURE AND ELECTROCHEMICAL BEHAVIOR**

BY

ERFAN SALAHINEJAD

THESIS

SUBMITTED TO THE SCHOOL OF GRADUATE STUDIES IN PARTIAL
FULFILLMENT OF THE REQUIREMENTS FOR THE DEGREE OF DOCTOR
OF PHILOSOPHY (Ph.D.)

IN

MATERIALS SCIENCE AND ENGINEERING

SHIRAZ UNIVERSITY

SHIRAZ, ISLAMIC REPUBLIC OF IRAN

EVALUATED AND APPROVED BY THE THESIS COMMITTEE: **EXCELLENT**

..... M.J. HADIANFARD, Ph.D. PROF. OF MATERIALS SCIENCE AND
ENGINEERING (CHAIRMAN)

..... M. PAKSHIR, Ph.D. ASSOCIATE PROF. OF MATERIALS SCIENCE
AND ENGINEERING

..... M.H. PAYDAR, Ph.D. ASSOCIATE PROF. OF MATERIALS SCIENCE
AND ENGINEERING

..... B. HASHEMI, Ph.D. ASSISTANCE PROF. OF MATERIALS SCIENCE
AND ENGINEERING

FEBRUARY 2013

Abstract

Production of nickel-free stainless steel coated with ZrTiO₄-PMMA hybrid sol–gel films and investigation of its structure and electrochemical behavior

By

Erfan Salahinejad

In this research, nickel-free austenitic stainless steels were prepared by mechanical alloying and liquid-phase sintering processes. According to X-ray diffraction and transmission electron microscopy, mechanical alloying of the powder mixture with the chemical composition of ASTM F2581, with iron nitride as the nitrogen source, produced nanocrystalline/amorphous powders. By liquid-phase sintering of the synthesized powder with a Mn-Si eutectic alloy as a novel additive, desirable densification was obtained. Also, X-ray diffraction and transmission electron microscopy showed that the austenite grain size remains yet in the nanometric scale even after the used sintering process at 1050 °C for 60 minutes. The corrosion behavior of the prepared stainless steels was studied by anodic potentiodynamic polarization and electrochemical impedance spectroscopy in a simulated body fluid, suggesting a better resistance compared with AISI 316L. Additionally, human stem cell adhesion evaluations on the synthesized implants confirmed their biocompatibility. In summary, the used mechanical alloying and sintering processes were found to be worthy to prepare nanostructured stainless steels with a high relative density and a desirable corrosion and cytocompatibility behavior. Afterwards, to improve the corrosion resistance and biocompatibility of the substrate, two types of sol–gel

derived thin films (ZrTiO_4 and hybrid ZrTiO_4 -PMMA) were deposited by a spin coating method. In the used particulate sol-gel process, a polymeric dispersant, namely carboxymethyl cellulose, was originally used to avoid agglomeration of nanoparticles and to obtain desirable film qualities. The films were characterized by differential scanning calorimetry, X-ray diffraction, transmission electron microscopy, atomic force microscopy, and scanning electron microscopy, indicating the preparation of high-coverage, crack-free, and homogeneous coatings. Water contact angle, electrochemical, and biocompatibility evaluations demonstrated that the coatings improve the hydrophilicity, corrosion resistance, and thereby biocompatibility of the substrate. Despite the higher corrosion protection by the hybrid ZrTiO_4 -PMMA coating, the sample coated with the pure ZrTiO_4 thin film exhibited a better cell viability. Furthermore, a new double-layer sol-gel coating, which comprises ZrTiO_4 as the bottom layer and ZrTiO_4 -PMMA as the top layer, was deposited on the stainless steel substrate. According to potentiodynamic polarization experiments, the substrate coated with this new film exhibited superior corrosion resistance, compared with the same steel coated with purely inorganic ZrTiO_4 and hybrid ZrTiO_4 -PMMA films. In summary, the ZrTiO_4 -based sol-gel films can be considered as an efficient approach to improving the corrosion resistance and biocompatibility of metallic implants.

Contents

Title	Page
1. Introduction	1
2. Theory and literature review	5
2.1. Biomaterials	6
2.1.1. An introduction to biomaterials	6
2.1.2. Metallic biomaterials	7
2.1.3. Corrosion of metallic implants	9
2.1.4. Surface modification of metallic biomaterials	9
2.1.5. Cytocompatibility (cell adhesion)	10
2.2. Nickel-free stainless steels	11
2.2.1. Biomedical nickel-free stainless steels	11
2.2.2. Other applications of nickel-free stainless steels	16
2.3. Powder metallurgy to synthesize stainless steels	18
2.3.1. An introduction to powder metallurgy	18
2.3.2. Mechanical alloying	19
2.3.3. Liquid-phase sintering	23
2.4. Nanostructured materials	25
2.4.1. An introduction to nanostructured materials	25
2.4.2. Corrosion behavior of nanostructured materials	26
2.5. Sol–gel method to prepare thin films	27
2.5.1. An introduction to sol–gel method	27
2.5.2. Sol–gel coating for corrosion protection	29
3. Experimental work and modeling.....	33
3.1. Stainless steel specimens	35
3.1.1. Mechanical alloying of stainless steel powders	35
3.1.2. Structural characterization of the milled powders	35
3.1.3. Sintering of the milled powders	36

3.1.4. Structural characterization of the sintered samples	37
3.1.5. Corrosion evaluation of the stainless steels	38
3.1.6. Modeling of the electrochemical data	39
3.1.7. Biocompatibility of the stainless steels	40
3.2. Sol–gel coatings	41
3.2.1. Sol–gel synthesis of nanoparticles	41
3.2.2. Structural characterization of the nanoparticles	42
3.2.3. Deposition of ZrTiO ₄ and ZrTiO ₄ -PMMA coatings	42
3.2.4. Structural characterization of the coatings	43
3.2.5. Properties of the sol–gel coated substrate	45
4. Results and discussion	46
4.1. Medical-grade stainless steels	47
4.1.1. Mechanical alloying of stainless steel powders	47
4.1.2. Sintering of the milled stainless steel powders	53
4.1.3. Corrosion evaluation of the stainless steels	62
4.1.4. Modeling of the EIS data for the stainless steels	69
4.1.5. Biocompatibility of the prepared stainless steels.....	73
4.2. Sol–gel coatings	76
4.2.1. Sol–gel synthesis of zirconium titanate nanoparticles ..	76
4.2.2. Numerical study of crystallization activation energy ...	80
4.2.3. Deposition of ZrTiO ₄ and ZrTiO ₄ -PMMA coatings	82
4.2.4. Electrochemical studies on the coated substrate	92
4.2.5. Modeling of the corrosion data for the coated samples	94
4.2.6. Inorganic–hybrid coated sample	98
4.2.7. Biocompatibility of the coated sample	99
5. Conclusions	103
6. Suggestions for future studies	106
References	108

Index of Tables

Caption Title	Page
Table 2-1. Chemical composition of ASTM stainless steels for surgical applications [11]	14
Table 3-1. Nominal ion concentration of SBF and blood plasma [66]... ..	38
Table 3-2. Classification of adhesion test results [70].....	44
Table 4-1. Results of the XRD analyses on the as-milled powders...	49
Table 4-2. Results of the XRD analyses on the 120 h milled powder heat-treated.....	53
Table 4-3. Chemical composition of the stainless steels (wt.%).....	63
Table 4-4. Some properties of the stainless steel samples.....	63
Table 4-5. Corrosion potential (E_{corr}), corrosion current density (j_{corr}), passive current density (j_p), and breakdown potential (E_b).....	66
Table 4-6. Common circuit elements.....	69
Table 4-7. Equivalent electrical circuit parameters obtained by the impedance studies.....	72
Table 4-8. Corrosion potential (E_{corr}), corrosion current density (j_{corr}), passive current density (j_p), and breakdown potential (E_b) of the coated samples.....	94
Table 4-9. Equivalent electrical circuit parameters obtained by the impedance studies.....	96
Table 4-10. Electrochemical data used for the porosity level calculation.....	97
Table 4-11. Corrosion potential (E_{corr}), corrosion current density (j_{corr}), passive current density (j_p), and breakdown potential (E_b) of the coated samples.....	99

Index of Figures

Caption Title	Page
Fig. 2-1. Clinical uses of inorganic biomaterials [3].....	7
Fig. 2-2. Percentage of allergy caused by each metallic element [5].....	8
Fig. 2-3. Schaeffler's phase diagram [13].....	13
Fig. 2-4. Pseudo binary phase diagram of a Fe-17Cr-10Mn-3Mo steel vs. its nitrogen content [16].....	15
Fig. 2.5. Schematic of the main factors affecting MA [34].....	21
Fig. 2-6. Sintering evolution of powder particles [44].....	23
Fig. 2-7. Two-dimensional model of a nanostructured material [50].....	26
Fig. 2-8. Hydrolysis and condensation in making sol-gel silica materials [55].....	29
Fig. 3.1. Schematic illustration of the thesis.....	34
Fig. 3.2. Schematic representation of powder densification.....	37
Fig. 3-3. Crosshatch pattern made on the coating for the adhesive test.....	44
Fig. 4-1. (a) XRD pattern of the milled steel powder, (b) XRD pattern and (c) fitting curve of the powder mixed with the standard.....	48
Fig. 4-2. (a) TEM micrograph and SAD pattern of the powder milled for 120 h; and (b) Related high-resolution TEM micrograph.....	50
Fig. 4-3. XRD pattern of the powder annealed at (a) 1150, (b) 1200, and (c) 1250 °C.....	53
Fig. 4-4. SEM image of the (a) milled steel and (b) additive powders.....	54
Fig. 4-5. Sintered densities measured by the Archimedes method.....	54
Fig. 4-6. Optical micrograph of the stainless steel samples containing (a) 0, (b) 3, and (c) 6 wt.% additive sintered at 1150 °C, indicating a	

progressive pore shrinkage and densification by increasing the additive content.....	55
Fig. 4-7. Optical micrograph of the samples containing 6 wt.% additive sintered at (a) 1000, (b) 1050, (c) 1100, and (d) 1200 °C.....	56
Fig. 4-8. (a) SEM micrograph and XMAP of (b) Fe, (c) Cr, (d) Mn, and (e) Si for the additive-containing specimen sintered at 1000 °C.....	58
Fig. 4-9. (a) SEM micrograph and XMAP of (b) Fe, (c) Cr, (d) Mn, and (e) Si for the additive-containing specimen sintered at 1050 °C.....	59
Fig. 4-10. (a) TEM micrograph and EDX analysis of regions A (b) and B (c) for the sample sintered at 1000 °C.....	60
Fig. 4-11. (a) XRD pattern, (b) TEM micrograph, and (c) high-resolution TEM micrograph of the additive-containing sample sintered at 1050 °C.....	61
Fig. 4-12. Optical micrograph of the sintered sample (a) before etching and (b) after etching in the Vilella's reagent.....	62
Fig. 4-13. Open circuit potential (<i>ocp</i>) vs. immersion time for the sample B.....	64
Fig. 4-14. Potentiodynamic polarization curves for the stainless steel samples.....	66
Fig. 4-15. (a) Bode impedance, (b) Bode phase angle and (c) Nyquist plots; and (d) equivalent electrical circuit.....	68
Fig. 4-16. Typical final fit for the (a) Bode and (b) Nyquist representation of Sample B.....	71
Fig. 4-17. Cell viability on the TCP and stainless steels after one day.....	74
Fig. 4-18. Low-magnification SEM micrograph of cells fixed on the sample B.....	74
Fig. 4-19. SEM micrograph of cells fixed on (a) A, (b) B, (c) C, and (d) 316L.....	75
Fig. 4-20. (a) TEM micrograph of the xerogel powder particles showing agglomeration, (b) that showing nanoparticles of 5 nm in size, and (c) the related SAD pattern.....	77

Fig. 4-21. TGA and DSC profiles of the xerogel.....	78
Fig. 4-22. XRD pattern of (a) the xerogel and the powders calcined at (b) 500, (c) 550, and (d) 600 °C.....	79
Fig. 4-23. (a) TEM micrograph and (b) SAD pattern of the powder calcined at 600 °C.....	80
Fig. 4-24. (a) DSC curves of ZrTiO ₄ crystallization obtained at the different heating rates and (b) related Kissinger plot.....	81
Fig. 4-25. SEM micrograph of the film deposited in the absence of CMC, (a) in a low magnification and (b) in a higher magnification.	83
Fig. 4-26. (a) SEM micrograph of the film obtained at a low magnification and SEM micrograph at higher magnifications obtained at a working voltage of (b) 20 kV and (c) 2 kV.....	83
Fig. 4-27. Optical photo of the (a) CMC-free and (b) CMC-containing sols after 2 weeks standing.....	85
Fig. 4-28. SEM micrograph of the (a) single-layer, (b) double-layer, and (c) triple-layer films.....	86
Fig. 4-29. (a) Thickness and (b) roughness values of the films.....	87
Fig. 4-30. Three-dimensional AFM image of the (a) single-layer, (b) double-layer, and (c) triple-layer zirconium titanate films.....	88
Fig. 4-31. SEM side-view image of the monolayer coated sample.	89
Fig. 4-32. (a) Low-magnification SEM, (b) high-magnification SEM, (c) three-dimensional AFM, and (d) two-dimensional AFM images of the hybrid film.....	90
Fig. 4-33. Water droplets on the stainless steel (a) uncoated and coated with the (b) ZrTiO ₄ and (c) ZrTiO ₄ –PMMA thin films.....	91
Fig. 4-34. SEM micrograph of the (a) inorganic and (b) hybrid coatings after the adhesive tape test. The arrow in b signifies a detached flake of the film.....	92
Fig. 4-35. Polarization curves of the coated samples.....	93
Fig. 4-36. (a) Bode impedance, (b) Bode phase angle, and (c) Nyquist plots; and (d) equivalent electrical circuit used for the quantitative analyses of the impedance spectra.....	95
Fig. 4-37. Typical fitting curve for the hybrid coating: (a) Bode and (b) Nyquist representation.....	96

Fig. 4-38. (a) Polarization curves of the samples coated with the sol-gel coatings; and SEM micrograph of the (b) hybrid and (c) inorganic-hybrid coatings after the polarization test.....	99
Fig. 4-39. Cell viability on the specimens after one day.....	100
Fig. 4-40. Low-magnification SEM micrograph of cells fixed on the stainless steel (a) uncoated and coated with the (b) $ZrTiO_4$ and (c) $ZrTiO_4$ -PMMA films.....	101
Fig. 4-41. SEM micrograph of cells fixed on the stainless steel (a) and coated with the (b) $ZrTiO_4$ and (c) $ZrTiO_4$ -PMMA thin films.....	101

Chapter 1

Introduction

1. Introduction

Metals and alloys are the oldest materials used in surgical purposes to make devices for fracture fixation, joint replacement, external splints, braces, and traction apparatus, as well as dental amalgams. Nowadays, the widely used metallic biomaterials include stainless steels, titanium and its alloys, cobalt-chromium-based alloys, as well as tantalum, niobium, and gold. Stainless steels, typically AISI 316L, are conventionally used in orthopedics, with main advantages of low cost, good mechanical properties, sufficient corrosion resistance, and easy processing. However, problems have been found with this type of medical-grade stainless steels. The most important problem is the negative effect of metal ions or fretting debris released from the implant due to corrosion and wear. Nickel and chromium are known as potentially harmful elements in the medical stainless steels. Nickel ions act as allergens in the human body, which may cause inflammations like swelling, reddening, eczema, and itching on skins. Due to the harmful effect of nickel ions on the human body, nickel-free austenitic stainless steels, generally Fe–Cr–Mn–Mo–N system, are considered as a potential replacement for conventional nickel-containing alloys. Because of this, with the development of new surgical stainless steels and the modification of ASTM medical standards, the nickel content is decreasing and the nitrogen content is increasing. Currently, in ASTM standards, two nickel-free medical-grade stainless steels are pointed out: ASTM F2229 and ASTM F2581.

To produce nitrogen-containing nickel-free austenitic stainless steels, there are several methods, such as melting processes, solid nitrogen absorption treatment, and powder metallurgy. It is known that mechanical alloying is a capable process to synthesize a wide variety of equilibrium and non-equilibrium structures, including supersaturated, metastable crystalline, quasicrystalline, intermetallic,

nanostructured, and amorphous alloy powders. This powder processing route can be successfully used to produce nitrogen-containing stainless steels. Nitrogen alloying through mechanical alloying can be accomplished by either milling under a reactive nitrogen atmosphere or milling under an inert atmosphere with metal nitrides. On the other hand, to meet the best mechanical and corrosion behaviors of powder metallurgy parts, high densities are imperative. To do so, a number of approaches like warm compaction, increasing sintering temperature and time, and using proper additives to activate liquid-phase sintering are under consideration. In the liquid-phase sintering process, the formation of a liquid phase promotes densification via providing a particle rearrangement, faster diffusion rate, and pore elimination.

In the biomaterials field, as well as the modification of the chemical composition of stainless steels, leading to the development of nitrogen-containing nickel-free alloys, surface modification techniques are considered, with the principal purpose of an improvement in corrosion resistance, wear resistance, antibacterial property, and tissue compatibility. Coating, as one of these methods, not only can increase the corrosion resistance of the implant, but also can improve the implant-tissue interaction, affecting biological responses like bioactivity and cytocompatibility. Among various methods used to process coatings, the sol–gel deposition process has advantages, such as high homogeneity, low sintering temperatures, and simplicity of complex shape coating.

In this thesis, medical-grade stainless steel powders with the nominal composition of ASTM F2581 were prepared by mechanical alloying. After powder characterization, bulk stainless steel samples were prepared by liquid-phase sintering of the same mechanically-alloyed powder with a Mn-Si eutectic alloy. Also, the corrosion behavior and cytocompatibility (stem cell adhesion) of the prepared samples were evaluated. Then, two types of sol–gel derived coatings (ZrTiO_4 and ZrTiO_4 -PMMA) were deposited on the stainless steel sample, to improve corrosion resistance and biocompatibility. Zirconium titanate (ZrTiO_4) and polymethyl methacrylate (PMMA) are known as a biocompatible ceramic and polymer, respectively. The

electrochemical behavior and cytocompatibility of the coated samples were also evaluated. Finally, the cell adhesion to the samples was correlated with surface characteristics of roughness, wettability, and corrosion resistance.

Chapter 2

Theory and literature review

2. Theory and literature review

2.1. Biomaterials

2.1.1. An introduction to biomaterials

Williams [1] defined biomaterials as “nonviable materials used in medical devices, intended to interact with the biological systems”. The basic requirement of a biomaterial is that the material and tissue environment should coexist without any undesirable effect on each other, defined as biocompatibility. These devices are termed as “implants” when they are intended to remain there for a substantial period, and as “prosthesis” when they are permanently fixed in the body for a long-term application until the end of lifetime [2]. Fig. 2-1 summarizes applications of inorganic biomaterials in the musculoskeletal system of the human body.

Orthopedic devices are generally implanted into the skeletal system of the human body for healing, correcting deformities, and restoring the lost functions of the original part. They are supporting bone plates, screws, total hip joints, knee joints, elbow joints, shoulder joints, and reattachments for tendons or ligaments. The implants are exposed to the biochemical and dynamic environment of the human body and their design is dictated by anatomy and restricted by physiological conditions. In the past few decades, the increase in the utilization of self-operating machines, participation of many persons in sports, defense activities, increased interest in motorcycles and bicycles, and day-to-day increasing traffic, have resulted in an enormous increase in the number of accidents. This has automatically led people to refer to orthopedic implants for the early recovery and resumption of their routine activities, which has provided a high level of motivation for the further development of orthopedic implants [3].

2.1.2. Metallic biomaterials

Metals and alloys are the oldest materials used in surgical purposes to make devices for fracture fixation, joint replacement, external splints, braces, and traction apparatus, as well as dental amalgams [3]. Because metals and alloys, compared to polymers and ceramics, have a more tensile strength, fatigue strength, and fracture toughness. Because of the critical and detrimental effects of corrosion on the human body, the history of metallic implants development has been mainly focused on better corrosion-resistant materials.

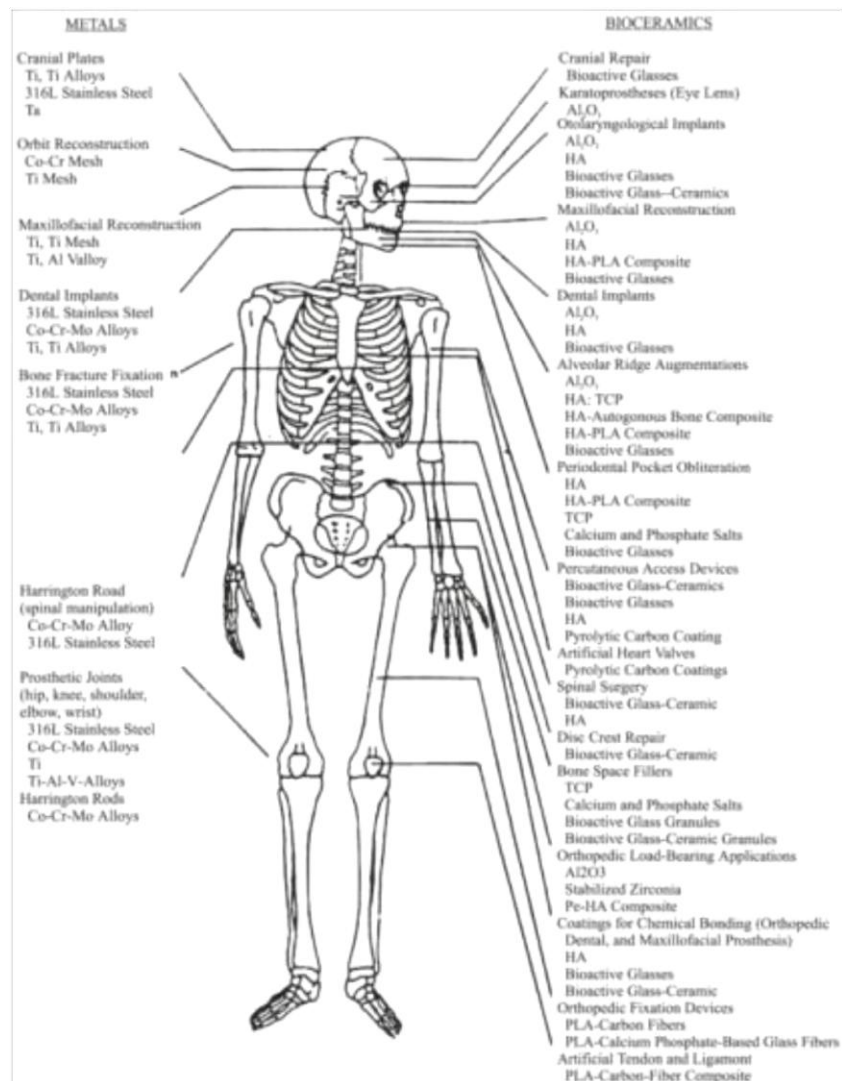


Fig. 2-1. Clinical uses of inorganic biomaterials [3].